Inorg. Chem. **2004**, *43*, 5550–5557

Self-Assembly Using Dynamic Coordination Chemistry and Hydrogen Bonding: Mercury(II) Macrocycles, Polymers and Sheets

Tara J. Burchell, Dana J. Eisler, and Richard J. Puddephatt*

Department of Chemistry, University of Western Ontario, London, Canada N6A 5B7

Received April 16, 2004

The self-assembly of extended metal-containing arrays is described based on dynamic coordination chemistry at mercury(II) with bis(amidopyridyl) ligands to form macrocycles, polymers, or sheets which can be further organized by hydrogen bonding between amide substituents. The ligands 1,2-$C_6H_4\{NHC(O)\text{-}4\text{-}C_5H_4N\}_2$, **1**, 1,2-$C_6H_4\{C(O)NHCH_2\text{-}4\text{-}C_5H_4N\}_2$, **2**, and 1,2-$C_6H_4\{CH_2C(O)NHCH_2\text{-}4\text{-}C_5H_4N\}_2$, **3** can adopt polar conformations and so can confer helicity in their complexes. Several macrocycles of formula $[(HgX_2)_2(\mu\text{-LL})_2]$ (LL = **1**, **2**), with tetrahedral mercury(II) centers, were prepared in which individual molecules are further self-assembled via hydrogen bonding in the solid state to form one- or two-dimensional polymers or sheets. In one case, a one-dimensional polymer $[\{(HgX_2)(\mu\text{-}\mathbf{3})\}_n]$ was formed. It is shown that the mercury(II) centers can be six-coordinate in forming the sheet structure $[\{(HgX_2)(\mu\text{-}\mathbf{2})_2\}_n]$, in which there are particularly large pores.

Introduction

The self-assembly of small building blocks to give macrocycles, polymers, networks and other complex supramolecular architectures, with potential uses as molecular materials, is a major area of research.[1,2] One particularly attractive method of constructing complex molecules is to use dynamic coordination chemistry, with labile metal centers and bridging ligands, to form the primary structure and then to use weaker, noncovalent interactions, such as hydrogen bonding, to organize these primary structures into supramolecular materials.[3] The inclusion of metal centers into supramolecular networks is potentially beneficial since the metal ions give access to physical and chemical properties that are not present in purely organic materials.[4] In addition, the metal ions may display a varying coordination number and varying stereochemistry, which can give rise to unusual topologies and can be used to increase the dimensionality of the self-assembled materials.[1−3]

Bridging bis(pyridyl) ligands are often used in the construction of metal-containing macromolecules, and the geometry of the bis(pyridyl) ligand can define the primary structure of the self-assembled macromolecule.[2] The incorporation of amide groups, which have known patterns of self-assembly through intermolecular hydrogen bonding, is less common but it has great potential in the organization of the primary molecules in the solid state.[5−8] The amide groups can often induce helicity in the macromeolecular structures and, since the final self-assembly through intermolecular hydrogen bonding is expected to mimic the hydrogen bonding in the parent bis(pyridyl) ligand, a degree of crystal

* Author to whom correspondence should be addressed. E-mail: pudd@uwo.ca. Fax: (519)661-3022.

(1) Steed, J. W.; Atwood, J. L. *Supramolecular Chemistry*; VCH: New York, 2000.

(2) (a) Holliday, B. J.; Mirkin, C. A. *Angew. Chem., Int. Ed.* **2001**, *40*, 2022. (b) Carlucci, L.; Ciani, G.; Proserpio, D. M. *Coord. Chem. Rev.* **2003**, *246*, 247. (c) Sweigers, G. F.; Malefeste, T. J. *Chem. Rev.* **2000**, *100*, 3483. (d) Leinninger, S.; Olenyuk, B.; Stang, P. J. *Chem. Rev.* **2000**, *100*, 853. (e) Beatty, A. M. *Coord. Chem. Rev.* **2003**, *246*, 131. (f) Roesky, H. W.; Andruh, M. *Coord. Chem. Rev.* **2003**, *236*, 91. (g) Mamula, O.; von Zelewsky, A. *Coord. Chem. Rev.* **2003**, *2426*, 87. (h) Ward, M. D.; McCleverty, J. A.; Jeffery, J. C. *Coord. Chem. Rev.* **2001**, *222*, 251. (i) Kaes, C.; Katz, A.; Hosseini, M. W. *Chem. Rev.* **2000**, *100*, 3553. (j) James, S. L. *Chem. Soc. Rev.* **2003**, 276. (k) Khlobystov, A. N.; Blake, A. J.; Champness, N. R.; Lemenovskii, D. A.; Majouga, A. G.; Zyk, N. V.; Schröder, M. *Coord. Chem. Rev.* **2001**, *222*, 155. (l) Batten, S.; Robson, R. *Angew. Chem., Int. Ed.* **1998**, *37*, 1460.

(3) (a) Raehm, L.; Mimassi, L.; Guyard-Duhayon, C.; Amouri, H. *Inorg. Chem.* **2003**, *42*, 5654. (b) Sailaja, S.; Rajasekharan, M. V. *Inorg. Chem.* **2003**, *42*, 5675. (c) Bhogala, B. R.; Thallapally, P. K.; Nangia, A. *Cryst. Growth Des.* **2004**, *4*, 215. (d) Tong, M.-L.; Wu, Y.-M.; Ru, J.; Chen, X.-M.; Chang, H.-C.; Kitagawa, S. *Inorg. Chem.* **2002**, *41*, 4846. (e) Qin, Z.; Jennings, M. C.; Puddephatt, R. J. *Inorg. Chem.* **2002**, *41*, 5174. (f) Brammer, L.; Rivas, J. C. M.; Atencio, R.; Fang, S.; Pigge, F. C. *J. Chem. Soc., Dalton Trans.* **2000**, 3855. (g) Aakeröy, C. B.; Beatty, A. M.; Lorimer, K. R. *J. Chem. Soc., Dalton Trans.* **2000**, 3869. (h) MacDonald J. C.; Dorrestein, P. C.; Pilley, M. M.; Foote, M. M.; Lundburg, J. L.; Henning, R. W.; Schultz, A. J.; Manson, J. L. *J. Am. Chem. Soc.* **2000**, 11692.

(4) (a) Bella, S. *Chem. Soc. Rev.* **2001**, *30*, 355. (b) Akutagawa, T.; Nakamura, T. *Coord. Chem. Rev.* **2002**, *226*, 3. (c) Sun, S.-S.; Less, A. J. *Coord. Chem. Rev.* **2002**, *230*, 171 (d) Janiak, C. *J. Chem. Soc., Dalton Trans.* **2003**, 2781.

10.1021/ic049500+ CCC: $27.50
Published on Web 07/24/2004

Chart 1

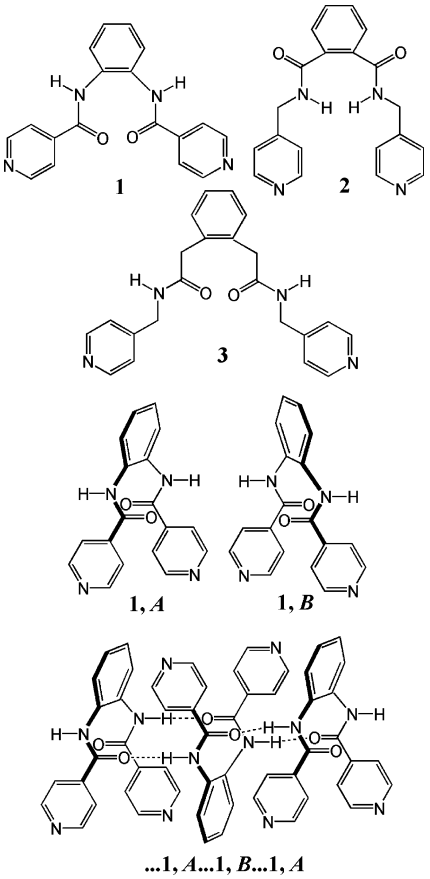

engineering is possible.[7] This approach can be considered as hierarchical or biomimetic, with the helicity and hydrogen bonding of the amide groups controlling the higher order structure in an analogous fashion to that found in many biological macromolecules.[5−8] The bis(pyridine) ligand 1,2-$C_6H_4\{NHC(O)\text{-}4\text{-}C_5H_4N\}_2$, **1** (Chart 1) was recently shown to form polymeric silver(I) or gold(I) complexes, with the formulae $[\{Ag(\mu\text{-}\mathbf{1})(\mu\text{-}X)\}_n]$ or $[\{Au_2(\mu\text{-}\mathbf{1})(\mu\text{-}\ Ph_2P(CH_2)_4\text{-}PPh_2)\}_n]^{2n+}$.[7] In the solid state, the ligand **1** exists in the chiral conformations ***A*** and ***B*** and alternating conformers are associated in an ..***A***..***B***..***A***..***B***.. fashion through intermolecular hydrogen bonds between amide groups of adjacent molecules (Chart 1). Both the silver(I) and gold(I) polymers $[\{Ag(\mu\text{-}\mathbf{1})(\mu\text{-}X)\}_n]$ and $[\{Au_2(\mu\text{-}\mathbf{1})(\mu\text{-}\ Ph_2P(CH_2)_4PPh_2)\}_n]^{2n+}$ underwent selfassembly in the solid state to form network structures through hydrogen bonding between amide units, and in each case the same ..***A***..***B***..***A***..***B***.. pattern as established in the free ligand **1** (Chart 1) was present.

Scheme 1

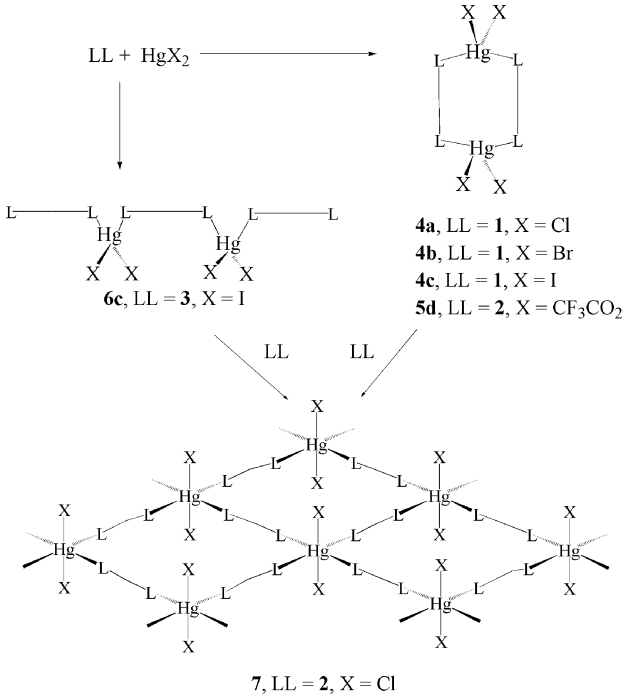

This article reports a series of mercury(II) complexes containing the bis(amidopyridine) ligands 1,2-$C_6H_4\{NHC(O)\text{-}4\text{-}C_5H_4N\}_2$, **1**; 1,2-$C_6H_4\{C(O)NHCH_2\text{-}4\text{-}C_5H_4N\}_2$, **2**; and 1,2-$C_6H_4\{CH_2C(O)NHCH_2\text{-}4\text{-}C_5H_4N\}_2$, **3** (Chart 1). The one or two extra methylene spacers in ligands **2** and **3**, respectively, lengthen the amido(pyridyl) arms and alter the geometry of the ligands with respect to **1**, thus giving the potential to form different architectures. While extended coordination networks derived from amidopyridyl ligands have been reported with the metal centers Ag(I), Au(I), Pd(II), and Pt(II),[5−7] the similar Hg(II) compounds have not been studied extensively.[8] A macrocyclic mercury(II) complex $[\{Hg(OAc)_2\}_2(\mu\text{-}1,1'\text{-bis}[(4\text{-pyridylamino})carbonyl]\text{-ferrocene})_2]$, with a bipyridyl bite distance N..N = 3.533 Å, was found to associate to form chains of macrocycles by intermolecular hydrogen bonding between N−H groups of the ligands and oxygen atoms of the trifluoroacetate groups.[8]

Results and Discussion

Reaction of equimolar amounts of the bis(amidopyridine) ligands **1**, **2**, or **3** (Chart 1) and mercury(II) halide or mercury(II) trifluoroacetate gave the corresponding complex $[HgX_2(\mu\text{-LL})]_n$, **4a**−**6d** (Scheme 1: **4**, LL = **1**; **5**, LL = **2**; **6**, LL = **3**; **a**, X = Cl; **b**, X = Br; **c**, X = I; **d**, X = CF_3CO_2). These complexes were isolated as analytically pure, air-stable, white solids that are very sparingly soluble in common organic solvents such as chloroform, dichloromethane, and tetrahydrofuran. The complexes **4a**, **4b**, **4c**, **5d**, and **6c** were characterized by X-ray structure determinations and the stoichiometry Hg:LL = 1:1 was confirmed in

(5) (a) Muthu, S.; Yip, J. H. K.; Vittal, J. J. *J. Chem. Soc., Dalton Trans.* **2002**, 4561. (b) Muthu, S.; Yip, J. H. K.; Vittal, J. J. *J. Chem. Soc., Dalton Trans.* **2001**, 3577. (c) Schauer, C. L.; Matwey, E.; Fowler, F. W.; Lauher, J. W. *J. Am. Chem. Soc.* **1997**, *119*, 10245. (d) Aakeröy, C. B.; Beatty, A. M. *Chem. Commun.* **1998**, 1067. (e) Aakeröy, C. B.; Beatty, A. M.; Desper, J.; O′Shea, M.; Valdés-Martínez, J. *J. Chem. Soc., Dalton Trans.* **2003**, 3956. (f) Qin, Z.; Jennings, M. C.; Puddephatt, R. J. *Chem. Eur. J.* **2002**, *8*, 735.

(6) (a) Qin, Z.; Jennings, M. C.; Puddephatt, R. J. *Inorg. Chem.* **2001**, *40*, 6220. (b) Qin, Z.; Jennings, M. C.; Puddephatt, R. J. *Chem. Commun.* **2001**, 2676. (c) Xu, X.; James, S. L.; Mingos, D. M. P.; White, A. J. P.; Williams, D. J.; *J. Chem. Soc., Dalton Trans.* **2000**, 3783. (d) Kuehl, C. J.; Tabellion, F. M.; Arif, A. M.; Stang, P. J. *Organometallics* **2001**, *20*, 1956.

(7) (a) Burchell, T. J.; Eisler, D. J.; Jennings, M. C.; Puddephatt, R. J. *Chem. Commun.* **2003**, 2228. (b) Burchell, T. J.; Eisler, D. J.; Jennings, M. C.; Puddephatt, R. J. *Chem. Commun.* **2004**, 944.

(8) (a) Li, G.; Song, Y.; Hou, H.; Li, L.; Fan, Y.; Zhu, Y.; Meng, X.; Mi, L. *Inorg. Chem.* **2003**, *42*, 913.

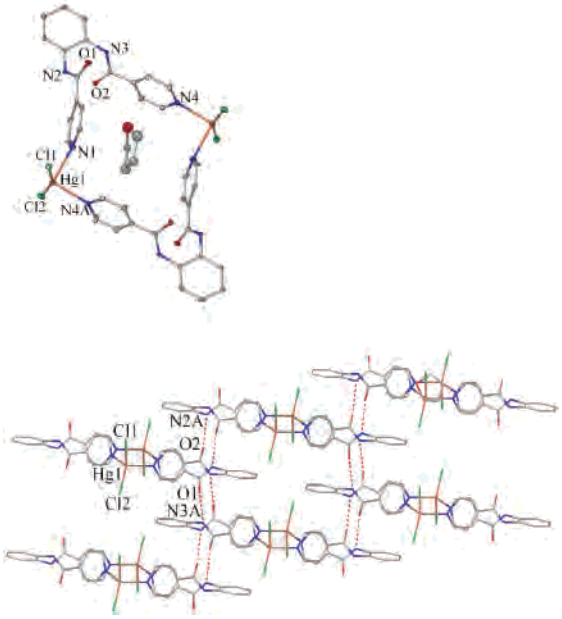

Figure 1. Top: View of the structure of macrocycle **4a**·THF. Bottom: 2-D network of rings formed by intermolecular hydrogen bonding between amide groups.

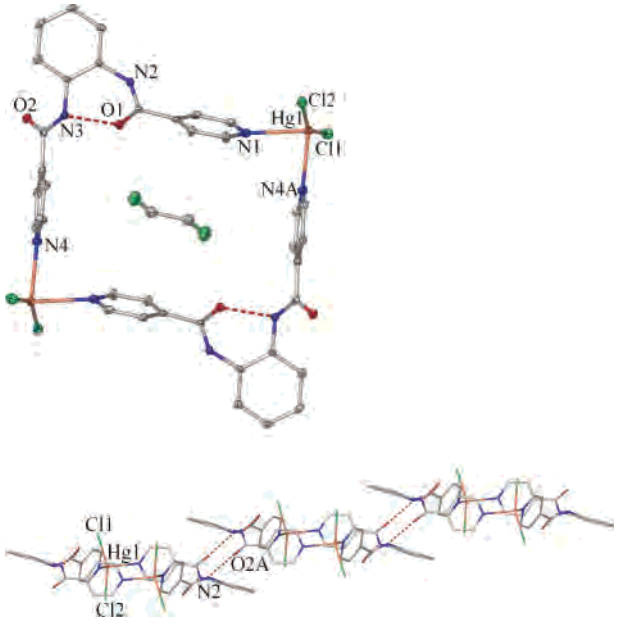

Figure 2. Top: View of the structure of macrocycle **4a**·DCE showing the intramolecular NH..O═C hydrogen bonding. Bottom: 1-D chain of rings formed by intermolecular hydrogen bonding between amide groups.

Table 1. Selected Bond Distances (Å) and Angles (°) for Macrocyclic Complexes **4a**−**4c**

	4a.2THF	**4a**.2DCE	**4b**.2THF	**4c**.2THF
Hg(1)−N(1)	2.526(8)	2.490(5)	2.445(5)	2.433(6)
Hg(1)−N(4A)	2.415(10)	2.407(5)	2.453(5)	2.467(6)
Hg(1)−X(1)	2.349(3)	2.351(1)	2.4800(9)	2.6444(6)
Hg(1)−X(2)	2.359(3)	2.369(1)	2.4743(9)	2.6523(6)
N(1)−Hg(1)−N(4A)	93.6(3)	84.7(2)	92.4(2)	90.3(2)
N(1)−Hg(1)−X(1)	93.6(2)	99.2(1)	99.8(1)	101.3(1)
N(4A)−Hg(1)−X(1)	102.5(2)	103.0(1)	99.4(1)	97.2(1)
N(1)−Hg(1)−X(2)	95.7(2)	92.9(1)	97.6(1)	102.2(1)
N(4A)−Hg(1)−X(2)	97.5(2)	102.0(1)	97.6(1)	101.5(1)
X(1)−Hg(1)−X(2)	157.4(1)	152.99(7)	155.01(3)	149.78(3)

each case. In the solid state, the complexes **4a**−**4c** exist as 30-membered macrocycles while **5d** exists as a 34-membered macrocycle, each having the formula $[(HgX_2)_2(\mu\text{-LL})_2]$ (LL = **1**, **2**). In contrast, complex **6c** forms a one-dimensional coordination polymer $[\{(HgCl_2)(\mu\text{-}\mathbf{3})\}_x]$ in the solid state (Scheme 1). Recrystallization of complex **5a** occurred with decomposition to give complex **7** (Scheme 1), which has the stoichiometry $[\{(HgCl_2)(\mu\text{-}\mathbf{2})_2\}_x]$, and which is shown to form an unusual sheet structure with 6-coordinate mercury(II) centers. Attempts were made to prepare other complexes with a 2:1 ligand-to-metal ratio, but **7** was the only one that was isolable. The complexes were characterized in solution by NMR and ESI−MS techniques, as described in the Experimental Section, but the NMR data did not clearly define the structures. In cases of dynamic coordination chemistry, it is seldom clear if the solid-state structures are maintained in solution.

Structures of the Macrocycles. The structure of complex **4a**, as the tetrahydrofuran solvate, is depicted in Figure 1, and selected bond distances and angles are listed in Table 1. In the complex **4a** there is a 30-membered macrocycle of the form $[(HgCl_2)_2(\mu\text{-}\mathbf{1})_2]$ with a (disordered) molecule of THF at the center (Figure 1, top). Each macrocycle contains two $HgCl_2$ units, with roughly tetrahedral stereochemistry at each mercury(II) center, and two bridging bis(amidopyridine) ligands **1** (see Table 1). The bite distance of the bipyridyl ligand N(1)..N(4) = 7.57 Å, and separation between the mercury centers (Hg(1)..Hg(1A) = 10.83 Å) is large enough to allow the macrocycle to accommodate one of two THF molecules of crystallization as a guest. In each macrocycle one ligand **1** is present in each of the chiral conformations ***A*** and ***B*** (Chart 1), and they are related by a center of symmetry. Individual molecules then self-assemble through pairwise NH..O═C hydrogen bonds between amide groups (N(2)..O(2A) = 2.89(1) Å, N(3)..O(3A) = 2.83(1) Å) to give a two-dimensional sheet structure (Figure 1, bottom). Thus, each ***A*** unit of the macrocycle is sandwiched between ***B*** units of two other macrocycles and *vice-versa*. This 2-D sheet structure results from crystal engineering of the macrocycles. Thus, the conformations and hydrogen bonding between the coordinated ligands in **4a** and in the free ligand **1** are very similar and so the nature of the self-assembly in **4a** was predictable.[7]

The structure of complex **4a** was also determined as the 1,2-dichloroethane (DCE) solvate. The structure is shown in Figure 2 and selected bond distances and angles are listed in Table 1. In the solid state, the complex is again present as a macrocycle $[(HgCl_2)_2(\mu\text{-}\mathbf{1})_2]$ and there is a molecule of DCE present as a guest at the center of the ring. However, there are some significant differences from the structure of the THF solvate of **4a**, as outlined below. The amide groups of each ligand **1** are more closely coplanar with the bridging phenylene group, and the conformation allows one intraligand NH..O═C hydrogen bond, N(3)..O(1) = 2.704(6) Å (Figure 2, top). In this conformation, the N..N bite distance is greater (N(1)..N(4) = 9.27 Å) and the mercury(II) centers are further apart (Hg(1)..Hg(1A) = 12.77 Å) than in the THF solvate. As a result, the cavity is distinctly more oblong than square in shape (compare Figure 2 (top) with Figure 1 (top)),

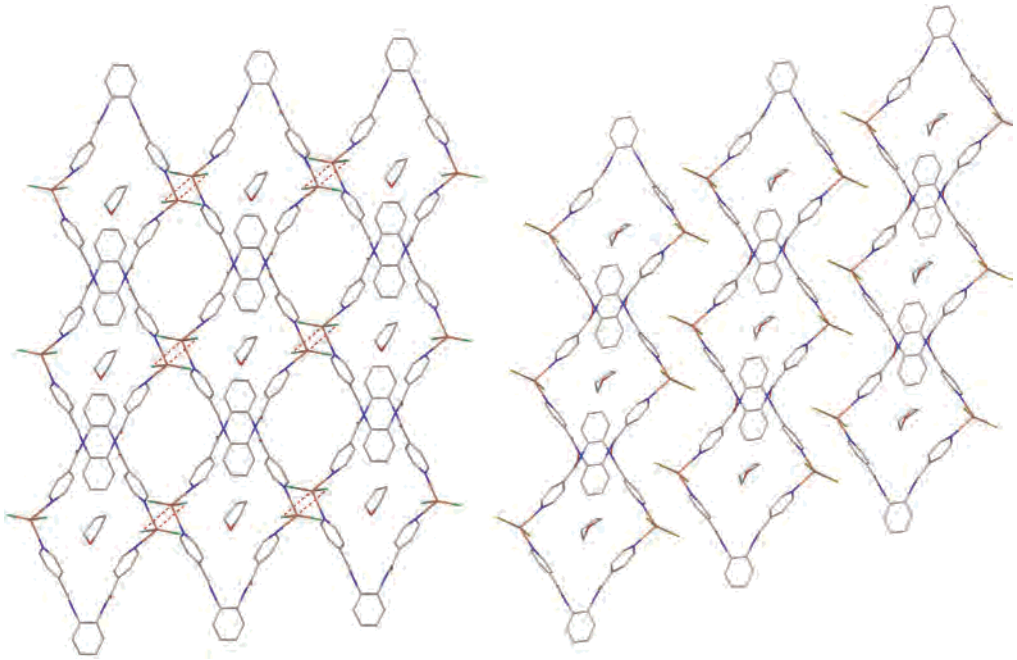

Figure 3. Comparison of the structures of complexes: (left) **4a**.THF and (right) **4c**.THF. In each case there are sheets of macrocycles with internal channels containing THF molecules. In **4a**.THF the sheets are crosslinked through pairwise Hg−Cl..Hg interactions, whereas in **4c**.THF there are no similar Hg−I..Hg interactions.

as required to accommodate the more linear DCE guest. Finally, since there is intramolecular hydrogen bonding, each macrocycle has only two available NH and C═O groups available for intermolecular hydrogen bonding. The result is that a one-dimensional polymer is formed through the intermolecular NH..O═C hydrogen bonding, which occurs between ***A***..***B*** conformer pairs (N(2)..O(2A) = 2.898(6) Å) as shown in Figure 2 (bottom), in contrast to the sheet structure of the THF solvate shown in Figure 1 (bottom). This appears to be a subtle case in which the guest molecule determines the conformation of the ligand **1**, which in turn determines the nature of the intermolecular self-assembly.[9]

The bromide and iodide complexes **4b** and **4c**, as the THF solvates, were isostructural and isomorphous with the corresponding chloride complex **4a**. Comparative structural data are included in Table 1. As expected, the cavity sizes are similar to that in **4a** (Hg(1)..Hg(1A) in **4a**: 10.83 Å, **4b**: 12.10 Å, **4c**: 12.00 Å) and the macrocycles self-assemble through hydrogen bonding between amide groups in the same way as in **4a** (**4b**: N(3)..O(1) = 2.772(6) Å, N(2)..O(2) = 2.786(6) Å; **4c**: N(3)..O(1) = 2.806(8) Å, N(2)..O(2) = 2.745(7) Å) to form two-dimensional sheets of rings. In each case, the sheets of macrocycles contain internal channels that contain the guest THF molecules as illustrated in Figure 3, but there are some differences. In particular, the chloride derivative **4a** (Figure 3, left) displays weak intersheet linking through pairwise, secondary Hg−Cl..Hg interactions (Hg..Cl = 3.22 Å) whereas the HgI_2 units in **4b** (Figure 3, right) are further offset such that there is no similar intersheet Hg−I..Hg interaction (Hg..I = 5.07 Å). The fact that these THF solvates all have the same macrocyclic structure and hydrogen-bonding motif and that the DCE solvate **4a**.DCE is different supports the view that the solvent inclusion determines the macrocyclic structure.

The structure of complex **5d** is shown in Figure 4 and selected bond distances and angles are listed in Table 2. The molecules of **5d** (Figure 4, top) exist as 34-membered macrocycles, $[(HgX_2)_2(\mu\text{-}\mathbf{2})_2]$, with $X = CF_3CO_2$. Compared to ligand **1**, ligand **2** has the amide groups inverted and it has two extra methylene spacer groups that give a correspondingly larger ring size in complexes **5** compared to **4**. However, the macrocycle **5d** is less planar than **4a**−**4c** and its cavity is considerably more narrow (N(1)..N(4) = 4.90 Å, Hg(1)..Hg(1A) = 4.62 Å), and two of the trifluoroacetate ligands are partially enclosed in the cavity, so there is no space for a guest molecule. Each macrocycle contains one ligand **2** in chiral conformation ***A*** and one in conformation ***B*** and the molecules selfassemble to form a two-dimensional sheet of rings (Figure 4, bottom), but in a different way compared to complexes **4**. In **5d** there is one typical intermolecular hydrogen bond between amide groups (N(3A)..O(1)═C = 2.979(8) Å) but the second intermolecular hydrogen bond is more complex. The N−H group of one amide substituent of ligand **2** is hydrogen bonded to a methanol solvent molecule (N(2)..O(70) = 2.893(9) Å), which in turn is hydrogen bonded to a trifluoroacetate group of a neighboring molecule NH..O(Me)H..O═C(CF_3)OHg (O..O = 2.814(8) Å), to provide intermolecular bridges and

(9) (a) Jetti, R. K. R.; Boese, R.; Thallapally, P. K.; Desiraju, G. R. *Cryst. Growth Des.* **2003**, *3*, 1033. (b) Withersby, M. A.; Blake, A. J.; Champness, N. R.; Cooke, P. A.; Hubberstey, P.; Li, W.-S.; Schröder M. *Inorg. Chem.* **1999**, *38*, 2259. (c) Lu, J.; Paliwala, T.; Lim, S. C.; Yu, C.; Niu, T.; Jacobson, A. J. *Inorg. Chem.* **1997**, *36*, 923. (d) Bu, X.-H.; Chen, W.; Hou, W.-F.; Du, M.; Zhang, R.-H.; Brisse, F. *Inorg. Chem.* **2002**, *41*, 3477. (e) Hennigar, T. L.; MacQuarrie, D. C.; Losier, P.; Rogers, R. D.; Zaworotko, M. J. *Angew. Chem., Int. Ed. Engl.* **1997**, *36*, 972. (f) Pedireddi, V. R.; Varughese, S. *Inorg. Chem.* **2004**, *43*, 450. (g) Thaimattam, R.; Xue, F.; Sarma, J. A. R. P.; Mak, T. C. W.; Desiraju, G. R. *J. Am. Chem. Soc.* **2001**, *123*, 4432.

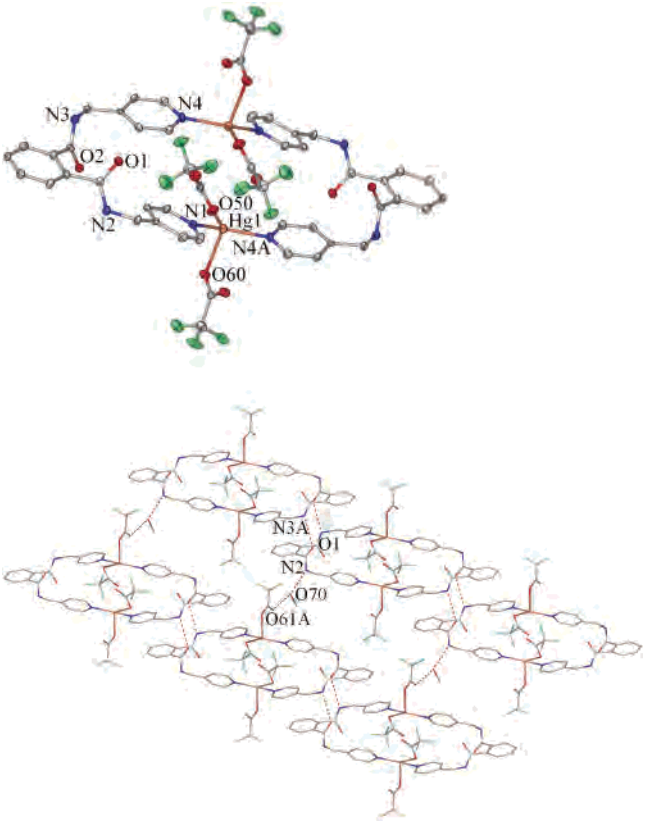

Figure 4. Top: View of the macrocyclic structure of complex **5d**. Bottom: 2-D network of rings of **5d** formed by a combination of amide..amide and amide..solvent..trifluoroacetate hydrogen bonds.

Table 2. Selected Bond Distances (Å) and Angles (°) for Macrocyclic Complex **5d**

Hg(1)−N(1)	2.168(6)	N(1)−Hg(1)−N(4A)	141.6(3)
Hg(1)−N(4A)	2.175(6)	N(1)−Hg(1)−O(50)	124.0(2)
Hg(1)−O(50)	2.383(6)	N(4A)−Hg(1)−O(50)	92.7(2)
Hg(1)−O(60)	2.400(6)	N(1)−Hg(1)−O(60)	100.8(2)
		N(4A)−Hg(1)−O(60)	94.8(2)
		O(50)−Hg(1)−O(60)	81.4(2)

so to form a chain of macrocycles in one direction. In addition, amide..amide hydrogen bonding occurs in an ***A***..***B***..***A***..***B*** manner to form a one-dimensional chain in a second direction. Together, the combination of the amide..amide and the more complex hydrogen bonding involving the trifluoroacetate, methanol, and N−H groups, forms the overall two-dimensional network. Thus, the solvate molecules of methanol play an important role in the final self-assembly process.

Structure of a Two-Dimensional Sheet Complex. The structure of complex **7** is shown in Figure 5 and selected bond distances and angles are listed in Table 3. Complex **7** crystallizes as $[(HgCl_2)(\mu\text{-}\mathbf{2})_2]_x$ in which each mercury(II) center has *trans* octahedral stereochemistry with $HgCl_2N_4$ coordination. Each bis(amidopyridine) ligand, **2**, bridges between two mercury(II) centers to generate the sheet structure shown in Figure 5 (top). These sheets contain 68-membered macrocyclic $(HgCl_2)_4(\mu\text{-}\mathbf{2})_4$ units. Each $HgCl_2$ unit is a node between four macrocycles and each ligand **2** forms an edge between two macrocycles. Each macrocycle has a saddle conformation in which the four $HgCl_2$ units are roughly coplanar with two bridging ligands below and two

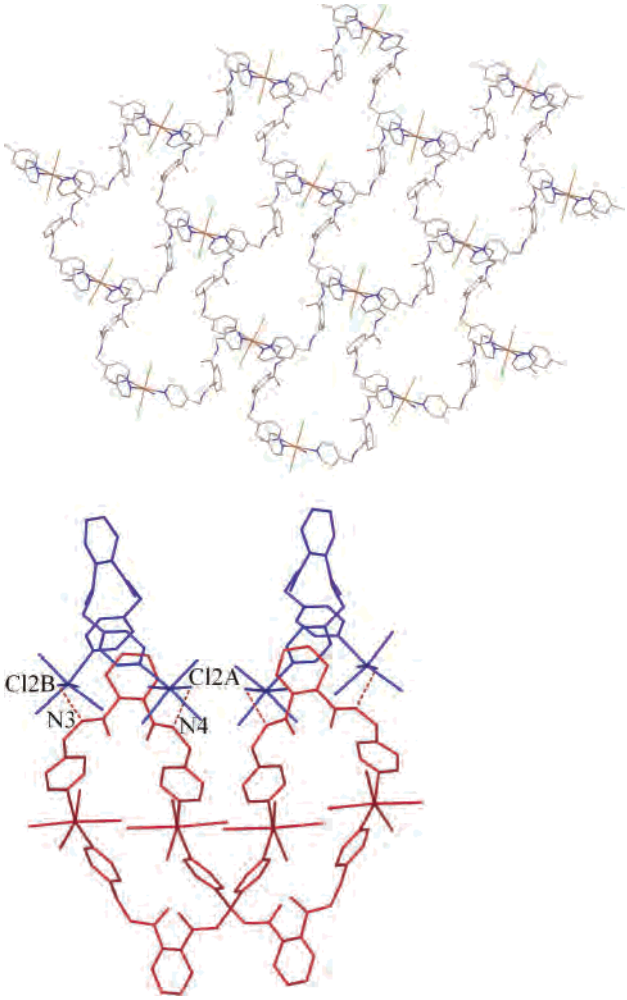

Figure 5. Top: View of the 2-D coordination network in complex **7**. Bottom: View of an individual macrocycle in complex **7** and NH..Cl hydrogen bonds between ***A*** and ***B*** sheets.

Table 3. Selected Bond Distances (Å) and Angles (°) for the Sheet Complex **7**

Hg(1)−N(2)	2.40(1)	N(2)−Hg(1)−N(2A)	85.7(6)
Hg(1)−N(5B)	2.34(1)	N(5B)−Hg(1)−Cl(2A)	84.7(3)
Hg(1)−Cl(2)	2.753(4)	N(5C)−Hg(1)−Cl(2A)	92.7(3)
N(5C)−Hg(1)−N(5B)	102.4(6)	N(2)−Hg(1)−Cl(2A)	99.8(4)
N(2)−Hg(1)−N(5B)	87.3(4)	N(2A)−Hg(1)−Cl(2A)	83.3(4)
N(2)−Hg(1)−N(5C)	164.8(5)	Cl(2A)−Hg(1)−Cl(2)	175.8(1)

above, as shown in Figure 5 (bottom). In the overall structure, there are equal numbers of ligands **2** in conformations ***A*** and ***B*** (Chart 1) but within each sheet all ligands have the same conformation ***A*** or ***B***. The neighboring sheets have ligands in opposite conformations in sequences ***A***..***B***..***A***..***B***. The ***A*** and ***B*** sheets are connected via intersheet hydrogen bonding of the N−H groups with chlorine atoms (N(3)..Cl(2) = 3.24(2) Å, N(4)..Cl(2) = 3.285(18) Å) (Figure 5, bottom). The overall structure can therefore be described as an intricate three-dimensional network, comprised of chiral sheets of interconnected macrocycles.

Structure of a Coordination Polymer. The structure of complex **6c** is shown in Figure 6 and selected bond distances and angles are listed in Table 4. Complex **6c** exists as the one-dimensional polymer $[\{(HgI_2)(\mu\text{-}\mathbf{3})\}_x]$ with tetrahedral mercury(II) centers bridged by the ligand **3**, which are again

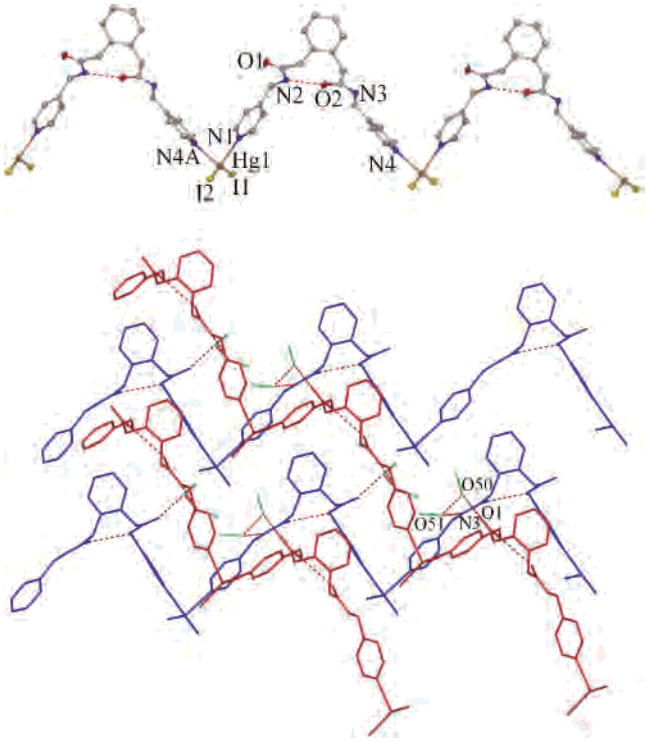

Figure 6. Top: View of the polymeric complex **6c** showing intramolecular NH..O═C hydrogen bonding. Bottom: Packing of polymer chains to give a double sheet structure with the sheets linked through NH..O(Me)-H..O(Me)H..O═C hydrogen bonding.

Table 4. Selected Bond Distances (Å) and Angles (°) for the Polymeric Complex **6c**

Hg(1)−N(1)	2.427(7)	N(1)−Hg(1)−N(4A)	96.4(2)
Hg(1)−N(4A)	2.408(7)	N(1)−Hg(1)−I(1)	103.12(18)
Hg(1)−I(1)	2.6601(9)	N(4A)−Hg(1)−I(1)	99.87(18)
Hg(1)−I(2)	2.6613(10)	N(1)−Hg(1)−I(2)	99.44(18)
		N(4A)−Hg(1)−I(2)	102.94(18)
		I(1)−Hg(1)−I(2)	148.70(3)

present in the chiral conformations ***A*** and ***B***. In this case, all ligands in a given polymer chain have the same conformation ***A*** or ***B*** and there are equal numbers of each form. There is an intraligand NH..O═C hydrogen bond for each bridging ligand **3** with N(2)..O(2) = 2.749(9) Å, as shown in Figure 6 (top). The ligand **3** clearly has a greater tendency than **1** or **2** to form polymers rather than rings (compare Figures 1−3 and Figure 6) and this difference is attributed to the extra methylene spacer groups in **3**. There are no great differences in the central ligand conformation in the ligand **3** compared to **1** and **2**, but the extra degrees of freedom of the longer bridging group favor polymer over macrocycle formation. The nonbonding distances N..N = 11.09 Å and Hg..Hg = 14.334 Å are correspondingly longer in **6c** than in the macrocycles **4**.

The arrangement of the polymer chains **6c** is shown in Figure 6 (bottom). The polymers are packed parallel to each other to give a sheet structure, in which all the polymer chains have the ligand in the same conformation ***A*** or ***B***. Pairs of all ***A*** and all ***B*** sheets are then linked together through solvent-mediated hydrogen bonding between amide groups of the kind NH..O(Me)H..O(Me)H..O═C. Since the ***A*** and ***B*** sheets have their polymer chains nonparallel (Figure 6, bottom), this long-range hydrogen bonding involving pairs of methanol molecules rigidifies the double sheet structure by crosslinking between different polymer chains. Relevant hydrogen bonding distances for the crosslinks are N(3)..O(51) of methanol = 2.87(1) Å, O(51)..O(50) of methanol = 2.66(2), and O(50)..O(1) =2.72(2).

Conclusions

It is shown that the reaction of mercury(II) compounds with bis(amidopyridine) ligands can give rise to complex structures by selfassembly. The bis(amidopyridine) ligands have a natural helicity and this is retained in the complexes that display several different ways of arranging the two chiral conformations ***A*** and ***B*** (Chart 1). In addition, the ligands are designed to participate in intermolecular hydrogen bonding to further organize the primary structures formed through dynamic coordination chemistry. The strategy has been successful in several instances, but complications can arise as a result of the different possible forms of hydrogen bonding. The most successful form of crystal engineering was found in the macrocyclic complexes such as **4a**.THF, which forms an unusual sheet structure with channels within the sheet that accommodate THF solvate molecules. In these complexes the hydrogen bonding pattern is the same as that found in the free ligand **1,** and so the form of self-assembly observed in the complexes was predicted. However, the ligands can adopt a conformation that allows intraligand NH···O═C hydrogen bonding, as observed in the macrocyclic complex **4a**.DCE (Figure 2) and in the polymer **6c** (Figure 6). Then, the intermolecular hydrogen bonding is more restricted, and was not readily predicted. In **4a**.DCE a one-dimensional polymer of macrocycles is formed while in **6c** the intermolecular hydrogen bonding is between amide NH and C═O groups, but mediated by pairs of methanol solvate molecules. In the beautiful sheet structure of complex **7**, the hydrogen bonding is of the form NH..Cl and this binds sheets of opposite chirality. It is likely that the Hg−Cl bonds are more polar in the octahedral $HgCl_2N_4$ units than in the more typical $HgCl_2N_2$ coordination and that this favors hydrogen bonding to the chloride rather than the carbonyl groups. In the macrocyclic trifluoroacetate derivative **5d**, there is one unit of the predicted intermolecular hydrogen bonding between amide units and another unit of hydrogen bonding involving an NH group and a trifluoroacetate ligand mediated by a molecule of methanol. The strategy of arranging the primary structure through hydrogen bonding between amide groups is successful in a good proportion of the cases studied, and the prospects of success are greatest when competing forms of hydrogen bonding are avoided.

Experimental Section

NMR spectra were recorded using a Varian Inova 400 NMR spectrometer. ^1H and ^{13}C chemical shifts are reported relative to tetramethylsilane (TMS).

1,2-C_6H_4(NHC(O)-4-$C_5H_4N)_2$, 1. Isonicotinic acid (2.460 g, 20.0 mmol) was refluxed in thionyl chloride (10 mL) for 2 h. Excess thionyl chloride was removed under vacuum leaving a colorless solid. The solid was suspended in tetrahydrofuran (40 mL) and then triethylamine (4.0 mL) and a solution of 1,2-phenylenediamine

(0.811 g, 7.50 mmol) in tetrahydrofuran (10 mL) were added. After refluxing for 1 h the mixture was allowed to cool, then it was poured into ice water. The resulting precipitate was filtered, washed with cold water, and dried. Washing with acetone purified the crude product. Yield 1.760 g, 74%. IR (KBr): ν(NH) 3289 cm^{-1}, ν(CH) 3050 cm^{-1}, ν(C═O) 1668 cm^{-1}. ^{1}H NMR (DMSO-d_6): 10.24 (s, 2H, NH); 8.77 (d, $^3J_{HH}$ = 6 Hz, 4H, H^{2,6} py); 7.85 (d, $^3J_{HH}$ = 5 Hz, 4H, H^{3,5} py); 7.67 (m, 2H, H^{4,5} Ph); 7.32 (m, 2H, H^{3,6} Ph); ^{13}C NMR: δ = 164.07 (C(O)), 150.32 (C^{2,6} py) 141.52 (C^4 py) 131.10 (C^{1,2} Ph), 126.22 (C^{3,6} Ph) 1295.91 (C^{4,5} Ph), 121.50 (C^{3,5} py). MS: *m*/*z* Calcd: 318.1116, Found: 318.1122.

1,2-C$_6$H$_4$(C(O)NHCH$_2$-4-C$_5$H$_4$N)$_2$, 2. NaH (0.180 g, 7.50 mmol) was added to a solution of 4-aminomethylpyridine (0.76 mL, 7.50 mmol) in tetrahydrofuran (30 mL) and the mixture was stirred for 30 min. The mixture was then cooled in a dry ice/acetone bath and a solution of phthaloyl dichloride (0.36 mL, 2.5 mmol) in tetradydrofuran (5 mL) was added dropwise over 15 min. The reaction mixture was allowed to warm to room temperature and then was stirred for 5 h. The crude product was collected by filtration, redissolved in CH_2Cl_2 and concentrated to 5 mL. Hexanes (20 mL) were added and the product, which precipitated out of solution, was collected by filtration. Yield 0.450 g, 52%. IR (KBr): ν(NH) 3231 cm^{-1}, ν(CH) 3069 cm^{-1}, ν(CH$_2$) 2932, 2894 cm^{-1}, ν(C═O) 1704, 1632 cm^{-1}. ^{1}H NMR (DMSO-d_6): 8.94 (t, $^3J_{HH}$ = 6 Hz, 2H, NH); 8.45 (d, $^3J_{HH}$ = 6 Hz, 4H, H^{2,6} py); 7.57 (m, 2H, H^{4,5} Ph); 7.53 (m, 2H, H^{3,6} Ph); 7.37 (d, $^3J_{HH}$ = 5 Hz, 4H, H^{3,5} py); 4.43 (d, $^3J_{HH}$ = 6 Hz, 4H, CH$_2$); ^{13}C NMR: δ = 168.48 (C(O)), 149.32 (C^{2,6} py) 148.45 (C^4 py) 136.18 (C^{1,2} Ph), 129.56 (C^{3,6} Ph) 127.63 (C^{4,5} Ph), 122.12 (C^{3,5} py) 41.54 (CH$_2$). MS: *m*/*z* Calcd: 346.1430, Found: 346.1423.

1,2-C$_6$H$_4$(CH$_2$C(O)NHCH$_2$-4-C$_5$H$_4$N)$_2$, 3. 1,2-phenylenediacetic acid (0.776 g, 4.00 mmol) was refluxed in thionyl chloride (10 mL) for 30 min. Excess thionyl chloride was removed under vacuum and the product was suspended in tetrahydrofuran (15 mL). The suspension was added dropwise to a tetrahydrofuran (30 mL) solution of 4-aminomethylpyridine (1.01 mL, 10 mmol,) and NaH (0.240 g, 10 mmol) that had been stirred for 1 h then cooled in a dry ice/acetone bath. The mixture was then allowed to warm to room temperature and was stirred for 3 h. Cold water was added to the reaction mixture and the product was collected by filtration and dried under vacuum. Yield 0.830 g, 55%. IR (KBr): ν(NH) 3313 cm^{-1}, ν(CH) 3081 cm^{-1}, ν(CH$_2$) 2924, 2855 cm^{-1}, ν(C═O) 1648 cm^{-1}. ^{1}H NMR (DMSO-d_6): 8.63 (t, $^3J_{HH}$ = 6 Hz, 2H, NH); 8.45 (s, br, 4H, H^{2,6} py); 7.25 (m, 2H, H^{4,5} Ph); 7.20−7.17 (m, 6H, H^{3,6} Ph, H^{3,5} py); 4.28 (d, $^3J_{HH}$ = 6 Hz, 4H, NHCH$_2$); 3.65 (s, 4H, CH$_2$C(O)); ^{13}C NMR: δ = 170.65 (C(O)), 149.42 (C^{2,6} py) 148.44 (C^4 py) 135.15 (C^{1,2} Ph), 130.06 (C^{3,6} Ph) 126.67 (C^{4,5} Ph), 122.05 (C^{3,5} py) 41.25 (NHCH$_2$) 39.61 (*C*H$_2$C(O)). MS: *m*/*z* Calcd: 374.1742, Found: 374.1732.

[{μ-1,2-C$_6$H$_4$(NHC(O)-4-C$_5$H$_4$N)$_2$}$_2$(HgCl$_2$)$_2$], 4a. $HgCl_2$ (0.0203 g, 0.075 mmol) was added to a solution of **1** (0.0238 g, 0.075 mmol) in CH_2Cl_2/methanol. After several minutes of stirring the complex precipitated out of solution as a white solid. The product was collected by filtration and dried under vacuum. Yield 0.0301 g, 68%. IR (KBr): ν(NH) 3269 cm^{-1}, ν(CH) 3059 cm^{-1}, ν(C═O) 1676 cm^{-1}. ^{1}H NMR (CD_2Cl_2/methanol-d_3): 10.19 (s, 2H, NH); 8.69 (d, $^3J_{HH}$ = 5 Hz, 4H, H^{2,6} py); 7.82 (d, $^3J_{HH}$ = 5 Hz, 4H, H^{3,5} py); 7.61 (m, 2H, H^{4,5} Ph); 7.34 (m, 2H, H^{3,6} Ph). Anal. Calcd (%) for $C_{18}H_{14}O_2N_4HgCl_2$·0.25 tetrahydrofuran: C: 39.66, H: 3.17, N: 8.81. Found: C: 39.75, H: 3.42, N: 8.76.

[{μ-1,2-C$_6$H$_4$(NHC(O)-4-C$_5$H$_4$N)$_2$}$_2$(HgBr$_2$)$_2$], 4b. This was prepared similarly from $HgBr_2$ (0.0270 g, 0.075 mmol,) and **1** (0.0238 g, 0.075 mmol). Yield 0.0361 g, 71%. IR (KBr): ν(NH) 3347, 3269 cm^{-1}, ν(CH) 3055 cm^{-1}, ν(C═O) 1674 cm^{-1}. ^{1}H NMR (CD_2Cl_2/methanol-d_3): 10.26 (s, 2H, NH); 8.67 (d, $^3J_{HH}$ = 5 Hz, 4H, H^{2,6} py); 7.82 (d, $^3J_{HH}$ = 5 Hz, 4H, H^{3,5} py); 7.60 (m, 2H, H^{4,5} Ph); 7.33 (m, 2H, H^{3,6} Ph). Anal. Calcd (%) for $C_{18}H_{14}O_2N_4HgBr_2$: C: 31.85, H: 2.07, N: 8.25. Found: C: 32.19, H: 1.83, N: 8.21.

[{μ-1,2-C$_6$H$_4$(NHC(O)-4-C$_5$H$_4$N)$_2$}$_2$(HgI$_2$)$_2$], 4c. This was prepared similarly from HgI_2 (0.0711 g, 0.150 mmol) and **1** (0.0477 g, 0.150 mmol). Yield 0.0773 g, 65%. IR (KBr): ν(NH) 3232 cm^{-1}, ν(CH) 3050 cm^{-1}, ν(C═O) 1667 cm^{-1}. ^{1}H NMR (CD_2Cl_2/methanol-d_3): 10.20 (s, 2H, NH); 8.69 (d, $^3J_{HH}$ = 5 Hz, 4H, H^{2,6} py); 7.82 (d, $^3J_{HH}$ = 5 Hz, 4H, H^{3,5} py); 7.61 (m, 2H, H^{4,5} Ph); 7.34 (m, 2H, H^{3,6} Ph). Anal. Calcd (%) for $C_{18}H_{14}O_2N_4HgI_2$: C: 27.97, H: 1.82, N: 7.25. Found: C: 28.18, H: 1.55, N: 7.07.

[{μ-1,2-C$_6$H$_4$(NHC(O)-4-C$_5$H$_4$N)$_2$}$_2${Hg(O$_2$CCF$_3$)$_2$}], 4d. This was prepared similarly from $Hg(O_2CCF_3)_2$ (0.0203 g, 0.075 mmol) and **1** (0.0238 g, 0.075 mmol). Yield 0.0301 g, 68%. IR (KBr): ν(NH) 3257 cm^{-1}, ν(CH) 3058 cm^{-1}, ν(C═O) 1670 cm^{-1}. ^{1}H NMR (CD_2Cl_2/methanol-d_3): 8.57 (d, $^3J_{HH}$ = 5 Hz, 4H, H^{2,6} py); 7.74 (d, $^3J_{HH}$ = 5 Hz, 4H, H^{3,5} py); 7.49 (m, 2H, H^{4,5} Ph); 7.22 (m, 2H, H^{3,6} Ph). Anal. Calcd (%) for $C_{22}H_{14}O_6N_4HgF_6$: C: 35.47, H: 1.89, N: 7.52. Found: C: 35.95, H: 2.15, N: 7.38.

[{μ-1,2-C$_6$H$_4$(C(O)NHCH$_2$-4-C$_5$H$_4$N)$_2$}$_2$(HgCl$_2$)$_2$], 5a. $HgCl_2$ (0.0271 g, 0.100 mmol) was added to a solution of **2** (0.0346 g, 0.100 mmol) in CH_2Cl_2/tetrahydrofuran. The solution was stirred for 30 min then hexane was added and the complex precipitated out of solution as a white solid. The product was collected by filtration and dried under vacuum. Yield 0.0391 g, 63%. IR (KBr): ν(NH) 3234 cm^{-1}, ν(CH) 3066 cm^{-1}, ν(CH$_2$) 2980, 2900 cm^{-1}, ν(C═O) 1634 cm^{-1}. ^{1}H NMR (CD_2Cl_2/methanol-d_3): 8.44 (d, $^3J_{HH}$ = 6 Hz, 4H, H^{2,6} py); 8.25 (t, $^3J_{HH}$ = 6 Hz, 2H, NH); 7.59 (m, 2H, H^{4,5} Ph); 7.53 (m, 2H, H^{3,6} Ph); 7.32 (d, $^3J_{HH}$ = 5 Hz, 4H, H^{3,5} py); 4.52 (d, $^3J_{HH}$ = 6 Hz, 4H, CH$_2$). Anal. Calcd (%) for $C_{20}H_{18}O_2N_4HgCl_2$·0.25 tetrahydrofuran: C: 39.66, H: 3.17, N: 8.81. Found: C: 39.75, H: 3.42, N: 8.76.

[{μ-1,2-C$_6$H$_4$(C(O)NHCH$_2$-4-C$_5$H$_4$N)$_2$}$_2$(HgBr$_2$)$_2$], 5b. This was prepared similarly from $HgBr_2$ (0.0360 g, 0.100 mmol) and **2** (0.0346 g, 0.100 mmol). Yield 0.0571 g, 81%. IR (KBr): ν(NH) 3247 cm^{-1}, ν(CH) 3059 cm^{-1}, ν(CH$_2$) 2922, 2858 cm^{-1}, ν(C═O) 1640 cm^{-1}. ^{1}H NMR (CD_2Cl_2/methanol-d_3): 8.38 (t, $^3J_{HH}$ = 6 Hz, 2H, NH); 8.35 (d, $^3J_{HH}$ = 6 Hz, 4H, H^{2,6} py); 7.30 (m, 2H, H^{4,5} Ph); 7.25 (m, 2H, H^{3,6} Ph); 7.13 (d, $^3J_{HH}$ = 6 Hz, 4H, H^{3,5} py); 4.32 (d, $^3J_{HH}$ = 6 Hz, 4H, CH$_2$). Anal. Calcd (%) for $C_{20}H_{18}O_2N_4HgBr_2$: C: 33.98, H: 2.56, N: 7.92. Found: C: 34.33, H: 2.58, N: 7.88.

[{μ-1,2-C$_6$H$_4$(C(O)NHCH$_2$-4-C$_5$H$_4$N)$_2$}$_2$(HgI$_2$)$_2$], 5c. This was prepared similarly from HgI_2 (0.0474 g, 0.100 mmol) and **2** (0.0346 g, 0.100 mmol). Yield 0.0544 g, 66%. IR (KBr): ν(NH) 3301, 3218 cm^{-1}, ν(CH) 3058 cm^{-1}, ν(CH$_2$) 2930, 2866 cm^{-1}, ν(C═O) 1655, 1639 cm^{-1}. ^{1}H NMR (CD_2Cl_2/methanol-d_3): 8.40 (t, $^3J_{HH}$ = 6 Hz, 2H, NH); 8.36 (d, $^3J_{HH}$ = 6 Hz, 4H, H^{2,6} py); 7.53 (m, 2H, H^{4,5} Ph); 7.47 (m, 2H, H^{3,6} Ph); 7.31 (d, $^3J_{HH}$ = 6 Hz, 4H, H^{3,5} py); 4.48 (d, $^3J_{HH}$ = 6 Hz, 4H, CH$_2$). Anal. Calcd (%) for $C_{20}H_{18}O_2N_4HgI_2$·CH_2Cl_2: C: 28.48, H: 2.28, N: 6.33. Found: C: 28.24, H: 2.09, N: 6.41.

[{μ-1,2-C$_6$H$_4$(C(O)NHCH$_2$-4-C$_5$H$_4$N)$_2$}$_2${Hg(O$_2$CCF$_3$)$_2$}$_2$], 5d. This was prepared similarly from $Hg(O_2CCF_3)_2$ (0.0426 g, 0.100 mmol) and **2** (0.0346 g, 0.100 mmol). The product crashed out of solution immediately upon addition of $Hg(O_2CCF_3)_2$. Yield 0.0515 g, 67%. IR (KBr): ν(NH) 3295 cm^{-1}, ν(CH) 3055 cm^{-1}, ν(CH$_2$) 2927, 2863 cm^{-1}, ν(C═O) 1650, 1613 cm^{-1}. ^{1}H NMR (CD_2Cl_2/methanol-d_3): 8.36 (d, $^3J_{HH}$ = 6 Hz, 4H, H^{2,6} py); 7.54 (m, 2H, H^{4,5} Ph); 7.48 (m, 2H, H^{3,6} Ph); 7.36 (d, $^3J_{HH}$ = 6 Hz, 4H, H^{3,5}

Table 5. Crystallographic Data for Complexes **4a**, **4b**, **4c**, **5d**, **6c**, and **7**

	4a·THF	**4a**·DCE	**4b**	**4c**	**5d**	**6c**	**7**
formula	$C_{44}H_{44}Cl_4Hg_2N_8O_6$	$C_{38}H_{32}Cl_6Hg_2N_8O_4$	$C_{44}H_{44}Br_4Hg_2N_8O_6$	$C_{44}H_{44}Hg_2I_4N_8O_6$	$C_{50}H_{44}F_{12}Hg_2N_8O_{14}$	$C_{25}H_{32}HgI_2N_4O_{4.25}$	$C_{41.5}H_{38}Cl_{3.5}HgN_8O_4$
fw	1323.85	1278.6	1501.69	1689.65	1610.11	910.94	1037.46
space group	*P*-1	*P*-1	*P*-1	*P*-1	*P*2(1)/c	*C*2/*c*	*P*-42(1)*c*
a (Å)	9.8328(20	9.0709(4)	9.3850(4)	9.3375(2)	15.8158(8)	26.824(5)	17.305(2)
b (Å)	10.9153(3)	10.4009(5)	12.2421(6)	12.1949(3)	12.3788(7)	10.116(2)	17.305(2)
c (Å)	12.2410(7)	11.5750(7)	12.9873(8)	13.2506(4)	14.9806(10)	24.316(5)	15.158(3)
α (°)	82.833(1)	81.207(2)	104.566(2)	104.646(2)	90	90	90
β (°)	74.783(1)	77.648(2)	103.513(2)	103.340(2)	110.784(2)	107.43(3)	90
γ (°)	81.504(2)	86.289(3)	111.298(3)	109.630(1)	90	90	90
volume (Å^3)	1248.73(8)	1053.65(9)	1255.11(11)	1289.84(6)	2742.1(3)	6295(2)	4539.4(1 3)
Z	1	1	1	1	2	8	4
D_{calc} (Mg/ m^3)	1.760	2.015	1.987	2.175	1.950	1.922	1.518
μ (mm^{-1})	6.406	7.708	9.345	8.389	5.706	6.886	3.645
R1, wR2 [I > 2σ(I)]	0.0610, 0.1196	0.0392, 0.0789	0.0465, 0.1014	0.0489, 0.1274	0.0568, 0.0870	0.0554, 0.1275	0.0845, 0.1756
R indices (all data)	0.1168, 0.1392	0.0522, 0.0838	0.0824, 0.1151	0.0661, 0.1389	0.1408, 0.1047	0.1176, 0.1502	0.1150, 0.1860

py); 4.50 (d, $^3J_{HH}$ = 6 Hz, 4H, CH_2). Anal. Calcd (%) for $C_{24}H_{18}O_6N_4HgF_6$: C: 37.29, H: 2.35, N: 7.25. Found: C: 37.22, H: 2.54, N: 7.17.

[{*μ*-1,2-C_6H_4($CH_2C(O)NHCH_2$-4-C_5H_4N)$_2$}$_x$($HgCl_2$)$_x$], 6a. $HgCl_2$ (0.0407 g, 0.150 mmol) was added to a solution of **3** (0.0564 g, 0.150 mmol) in tetrahydrofuran/methanol. The product precipitated out of solution after several hours of stirring and was collected by filtration and dried under vacuum. Yield 0.0577 g, 59%. IR (KBr): ν(NH) 3269 cm^{-1}, ν(CH) 3078 cm^{-1}, ν(CH_2) 2950, 2896 cm^{-1}, ν(C═O) 1649 cm^{-1}. ^{1}H NMR (CD_2Cl_2/methanol-d_3): 8.37 (d, $^3J_{HH}$ = 6 Hz, 4H, $H^{2,6}$ py); 8.25 (t, $^3J_{HH}$ = 6 Hz, 2H, NH); 7.31 (m, 2H, $H^{4,5}$ Ph); 7.27 (m, 2H, $H^{3,6}$ Ph); 7.15 (d, $^3J_{HH}$ = 6 Hz, 4H, $H^{3,5}$ py); 4.34 (d, $^3J_{HH}$ = 6 Hz, 4H, $NHCH_2$); 3.68 (s, 4H, $CH_2C(O)$). Anal. Calcd (%) for $C_{22}H_{22}O_2N_4HgCl_2$: C: 40.91, H: 3.43, N: 8.67. Found: C: 41.26, H: 3.41, N: 8.59.

[{*μ*-1,2-C_6H_4($CH_2C(O)NHCH_2$-4-C_5H_4N)$_2$}$_x$($HgBr_2$)$_x$], 6b. This was prepared similarly from $HgBr_2$ (0.0753 g, 0.150 mmol) and **3** (0.0564 g, 0.150 mmol). Yield 0.0721 g, 65%. IR (KBr): ν(NH) 3279 cm^{-1}, ν(CH) 3063 cm^{-1}, ν(CH_2) 2923, 2859 cm^{-1}, ν(C═O) 1655 cm^{-1}. ^{1}H NMR (CD_2Cl_2/methanol-d_3): 8.42 (t, $^3J_{HH}$ = 6 Hz, 2H, NH); 8.33 (d, $^3J_{HH}$ = 6 Hz, 4H, $H^{2,6}$ py); 7.29 (m, 2H, $H^{4,5}$ Ph); 7.25 (m, 2H, $H^{3,6}$ Ph); 7.10 (d, $^3J_{HH}$ = 6 Hz, 4H, $H^{3,5}$ py); 4.31 (d, $^3J_{HH}$ = 6 Hz, 4H, $NHCH_2$); 3.67 (s, 4H, $CH_2C(O)$). Anal. Calcd (%) for $C_{22}H_{22}O_2N_4HgBr_2$·0.25 tetrahydrofuran: C: 36.69, H: 3.21, N: 7.44. Found: C: 36.63, H: 3.54, N: 7.17.

[{*μ*-1,2-C_6H_4($CH_2C(O)NHCH_2$-4-C_5H_4N)$_2$}$_x$(HgI_2)$_x$], 6c. This was prepared similarly from HgI_2 (0.0908 g, 0.200 mmol) and **3** (0.0753 g, 0.200 mmol). Yield 0.0711 g, 43%. IR (KBr): ν(NH) 3282 cm^{-1}, ν(CH) 3063 cm^{-1}, ν(CH_2) 2918, 2858 cm^{-1}, ν(C═O) 1652 cm^{-1}. ^{1}H NMR (CD_2Cl_2/methanol-d_3): 8.40 (t, $^3J_{HH}$ = 6 Hz, 2H, NH); 8.36 (d, $^3J_{HH}$ = 6 Hz, 4H, $H^{2,6}$ py); 7.29 (m, 2H, $H^{4,5}$ Ph); 7.25 (m, 2H, $H^{3,6}$ Ph); 7.15 (d, $^3J_{HH}$ = 6 Hz, 4H, $H^{3,5}$ py); 4.33 (d, $^3J_{HH}$ = 6 Hz, 4H, $NHCH_2$); 3.68 (s, 4H, $CH_2C(O)$). Anal. Calcd (%) for $C_{22}H_{22}O_2N_4HgI_2$: C: 31.88, H: 2.68, N: 6.76. Found: C: 32.30, H: 3.06, N: 6.29.

[{*μ*-1,2-C_6H_4($CH_2C(O)NHCH_2$-4-C_5H_4N)$_2$}$_x${Hg(O_2CCF_3)$_2$}$_x$], 6d. This was prepared similarly from $Hg(O_2CCF_3)_2$ (0.064 g, 0.150 mmol), **2** (0.0564 g, 0.150 mmol). Yield 0.0874 g, 72%. IR (KBr): ν(NH) 3293 cm^{-1}, ν(CH) 3075 cm^{-1}, ν(CH_2) 2923, 2853 cm^{-1}, ν(C═O) 1658, 1624 cm^{-1}. ^{1}H NMR (CD_2Cl_2/methanol-d_3): 8.36 (s, br, 4H, $H^{2,6}$ py); 7.33 (s, br, 2H, $H^{4,5}$ Ph); 7.30−7.21 (m, 6H, $H^{3,6}$ Ph, $H^{3,5}$ py); 4.39 (d, $^3J_{HH}$ = 6 Hz, 4H, $NHCH_2$); 3.74 (s, 4H, $CH_2C(O)$). Anal. Calcd (%) for $C_{26}H_{22}O_6N_4HgF_6$: C: 38.98, H: 2.77, N: 6.99. Found: C: 38.56, H: 3.06, N: 6.50.

X-ray Structure Determinations. A crystal suitable for X-ray analysis was mounted on a glass fiber. Data were collected using a Nonius-Kappa CCD diffractometer using COLLECT (Nonius, B. V. 1998) software. The unit cell parameters were calculated and refined from the full data set. Crystal cell refinement and data reduction was carried out using the Nonius DENZO package. The data were scaled using SCALEPACK (Nonius, B. V. 1998). The SHELX-TL V5.1 and SHELX-TL V6.1 (Sheldrick, G. M.) program packages were used to solve and refine the structures. The structures of **4b**, **7**, and **6c** were solved by direct methods, while complexes **4a**, **4c**, and **5d** were solved by the automated Patterson routine of the SHELX-TL software package. Crystal data are summarized in Table 5. All thermal ellipsoid diagrams are shown at 30% probability.

Acknowledgment. We thank NSERC and EMK (Canada) for financial. T.J.B. thanks NSERC for a scholarship and R.J.P. thanks the government of Canada for a Canada Research Chair.

Supporting Information Available: Crystallographic data in CIF format. Figures showing thermal ellipsoid plots of the fundamental or asymmetric units in the crystals. This material is available free of charge via the Internet at http://pubs.acs.org.

IC049500+